

Review Article

Phase Behavioral Effects on Particle Formation Processes Using Supercritical Fluids

Srinivas Palakodaty^{1,3} and Peter York^{1,2}

Received November 4, 1998; accepted February 16, 1999

The application of supercritical fluid (SF) processing in pharmaceutical research is increasing particularly in the field of particle formation for drug delivery systems. The SF processes have benefits over the existing particle formation methods in terms of improved control, flexibility and operational ease. This review highlights the fundamental concepts of fluid phase behaviour and their influence on the various processes involving particle formation with supercritical fluids. Several phase behaviour systems are discussed to provide an insight into the factors influencing the process paths and their effects on the characteristics of the particles.

KEY WORDS: pharmaceuticals; materials processing; supercritical fluid processing; particles.

INTRODUCTION

The production of particles with specific physicochemical properties for targeted drug delivery is a constant challenge in the pharmaceutical industry. This is especially problematic for micron and submicron sized particles. The deployment of supercritical fluids as a means for particle formation offers promise. Currently, supercritical fluids (SF) have been successfully used in preparing pharmaceuticals, proteins, polymers/bio polymers and inorganic materials in micron sized or submicron sized particles with alternative morphological and solid state forms. While disadvantages associated with some of the classical particle formation operations such as spray drying and jet milling are absent with supercritical fluid processing, the area is relatively new with minimal scientific theory supporting the various processes.

The different recrystallization methods using supercritical fluids currently reported can be broadly classified into three categories (i) precipitation from supercritical solutions (ii) precipitation from saturated solutions using supercritical fluid as an antisolvent and (iii) precipitation from gas saturated solutions. These processes are described in detail below along with the new improved methods which have recently emerged. However, in parallel to considering these processes, it is important to consider the phase behaviour of different supercritical fluid systems. This review illustrates some of the basic underlying thermodynamic principles of fluid phase equilibria near the critical conditions and their possible influences on the different

SF crystallisation processes. A thorough understanding is essential when manipulating the experimental conditions to achieve changes in the crystallisation mechanism in a controlled manner to obtain a product with targeted properties.

PHASE BEHAVIOR

Single Component System

A pure substance can exist in three different states of matter—solid, liquid or gas dictated by the two independent variables temperature and pressure—as shown in Fig. 1a. Equilibrium between different phases is along the saturation curves and the three phases co-exist in equilibrium at the triple point. The vaporisation curve ends at the critical point representing the maximum temperature and pressure where the liquid and vapour phases can coexist in equilibrium with each other. The state of fluid at temperatures and pressures above the critical point is referred to as supercritical fluid or compressed gas due to high compressibility. Their physical and transport properties vary between those of liquids and gases. The variation in density and viscosity of carbon dioxide with pressure at 310 K is shown in Fig. 1b.

BINARY SYSTEM

Solid-Fluid

Unlike gases at low pressures, supercritical fluids show remarkable solvent power for high molecular weight, low vapour pressure solids, which can be varied over a wide range by altering pressure and/or temperature. Figure 2 shows the solubility changes of nifedipine in supercritical carbon dioxide. The solubility increases with increasing pressure at all temperatures. The effect of temperature at constant pressure is quite different, due to the vapour pressure changes of the solute.

¹ Bradford Particle Design Limited, 49, Listerhills Science Park Campus Road, Bradford BD7 1HR, UK.

² Drug Delivery Group, Pharmaceutical Technology, School of Pharmacy, University of Bradford, Bradford BD7 1DP, UK.

³ To whom correspondence should be addressed. (e-mail: s.palakodaty@bradford.ac.uk)

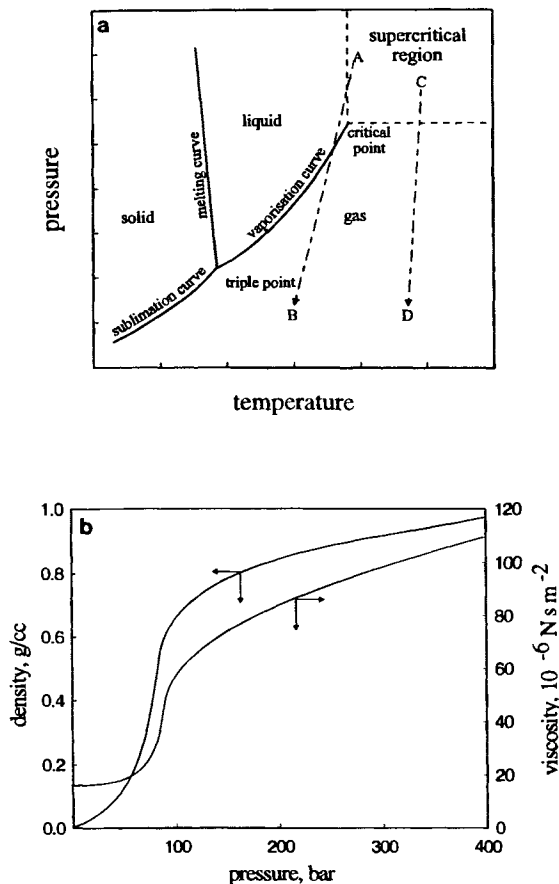


Fig. 1 (a) P-T diagram of a one component system. (b) Density and viscosity variation of carbon dioxide with pressure at 310 K. (density data from Angus *et al.* (2) and viscosity data from Stephan and Lucas (3)).

The solubility decreases with increasing temperatures up to pressures below the cross over region, which is about 220 bar for this system, and then increases. A detailed description of the various types of phase behaviour with solid-SF systems is available (1). Further, the solubility of solids in SF's in general,

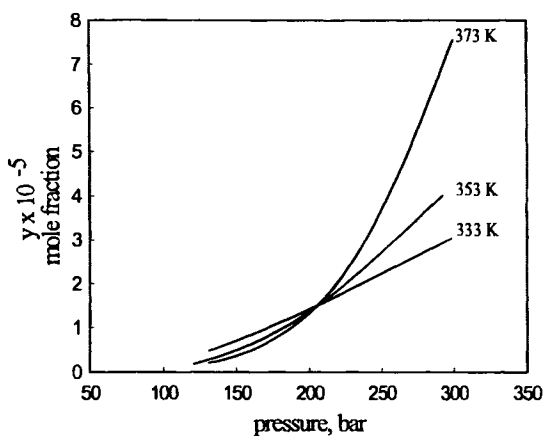


Fig. 2. Solubility of nifedipine (dimethyl 1,4-dihydro-2,6-dimethyl-4-(o-nitrophenyl)-3,5-pyridinedicarboxylate) in supercritical carbon dioxide (data from Knez *et al.* (9)).

is enhanced by the addition of a small amount of organic modifier (4-6). The solubilities of several pharmaceutical compounds in pure and modified SF have been reported recently (7-9) and reviews of studies covering the solubilities of various pharmaceuticals in SF's have been presented (10-11).

LIQUID-VAPOR/SF

Figure 3a shows a simple type I phase behaviour of carbon dioxide-ethanol binary vapour liquid system at 308 K and 333 K. The binodal curve represents the boundaries of the vapour-liquid equilibrium. The solubility of carbon dioxide in ethanol increases sharply with pressure while the solubility of ethanol in carbon dioxide remains more or less constant. The saturated liquid and vapour curves meet at the mixture critical point. At pressures above the mixtures' critical point, the two fluids are completely miscible. In the miscibility region, for example at 308 K, a mixture with a composition corresponding to A is rich in ethanol and that corresponding to B is rich in carbon dioxide. The high solubility of gas decreases the ethanol density dramatically as shown by the density changes in the respective phases in Fig. 3b. A more comprehensive description of the various types of phase behaviour is detailed by McHugh and Krukonic (1). Several sources of vapour liquid equilibrium data are available (14-17).

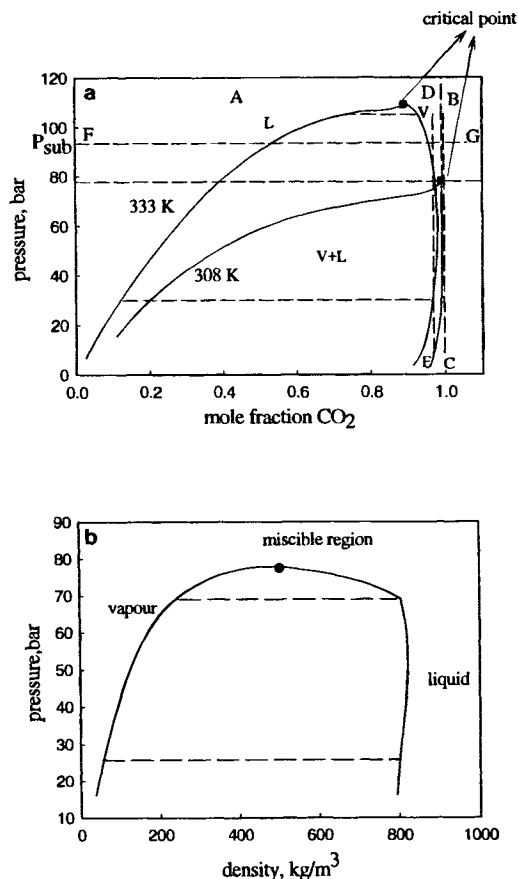


Fig. 3. (a) Binary vapor-liquid equilibrium of ethanol-carbon dioxide system. (data at 308 K from Tanaka and Kato (12) and at 333 K from Suzuki *et al.* (13)). (b) Densities for CO₂-ethanol system at 308 K. (data from Tanaka and Kato (12)).

TERNARY SYSTEM

Water-Organic Solvent-Vapor/SF

Unlike a two phase binary system, a two phase ternary system has three degrees of freedom and hence is usually best represented at constant temperature and pressure. A typical three component system of carbon dioxide-ethanol-water at 308 K is shown in Fig. 4. At 69 bar, i.e., at a pressure below the binary mixture critical point ($P_{CM} = 80$ bar, see Fig. 4), carbon dioxide and ethanol exist in two phases. The equilibrium compositions in the respective phases are shown on the CO_2 -ethanol line in Fig. 4a. Water and CO_2 also exist as two phases and their equilibrium compositions are shown on the CO_2 -water line. Ethanol and water are completely miscible at 308 K and 69 bar. The ternary mixture exists in two phases bounded by the saturated liquid and vapour curves as shown in Fig. 4a. The single phase vapour region is very narrow as compared to the liquid phase region. As the pressure is raised above the critical pressure of CO_2 -ethanol binary mixture, the two fluids are completely miscible and the two phase boundary is enveloped by a binodal curve as shown in Fig. 4b at 102 bar. The point where the saturated vapour and liquid curve meet, i.e., the point where all the three fluids are completely miscible, is often referred to as plait point and is the mixture critical point. A mixture in the liquid region is rich in ethanol + water and in the vapour region is rich in carbon dioxide. More comprehensive description of various types of phase behaviour with aqueous systems is available (1,20). Vapour liquid equilibrium data of several ternary systems are reported in the literature (14,16-17).

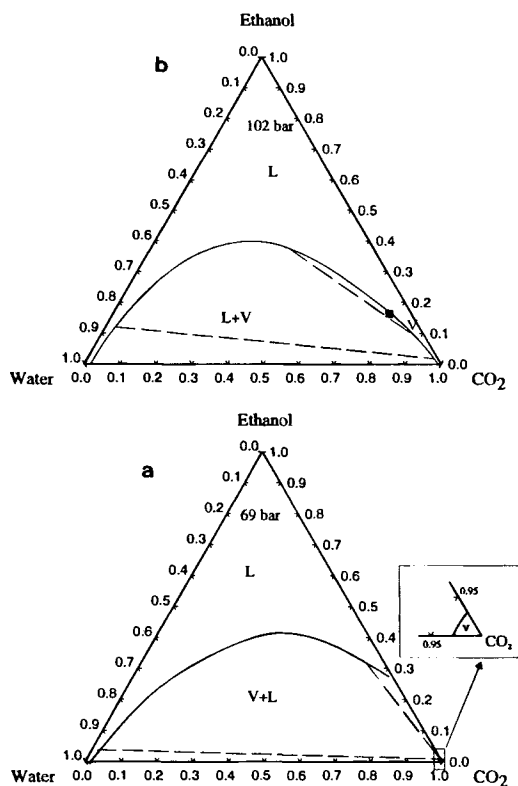


Fig. 4. Phase equilibria of the ternary system carbon dioxide-ethanol-water at 308 K. (data at 102 bar from Gilert and Paulaitis (18) and at 69 bar from Yao *et al.* (19))

SOLUTE-ORGANIC SOLVENT-VAPOR/SF

Solids processing using supercritical fluids often involves such systems and hence is most relevant to supercritical fluid crystallisation methods. No study to date has appeared in the literature which provides the complete phase behaviour of organic solids and liquids in the presence of a supercritical fluid at constant temperature and pressure. Figure 5 shows a simple representative phase behaviour of a ternary system at constant temperature and pressure containing a supercritical fluid. When the lighter component of the system is in a vapour state, the system can exhibit 6 regions of coexisting phases—(a) liquid (b) vapour-liquid (c) liquid-solid (d) vapour-liquid-solid (e) vapour-solid and (f) a homogenous vapour phase, and these are shown in Fig. 5a. At pressures above the critical point of the binary organic solvent-SF mixture, the number of coexisting phases reduces to four as shown in Fig. 5b. The solubility of solid in SF is in general low compared to that of solid in solvent and solvent in SF.

POLYMER-ORGANIC SOLVENT-SF

The glass transition temperature of glassy polymers is substantially lowered by the adsorption of supercritical fluid and subsequent swelling of the polymer. Wissinger and Paulaitis (21) report a 70% reduction in the glass temperature of PMMA and polystyrene polymers in the presence of SF CO_2 . Accordingly, the phase behaviour of a binary polymer-SF and a ternary polymer-solvent-SF system is complex and a simple representation is shown in Fig. 6. Figure 6a shows a binodal curve encompassing a two phase metastable region and an unstable two

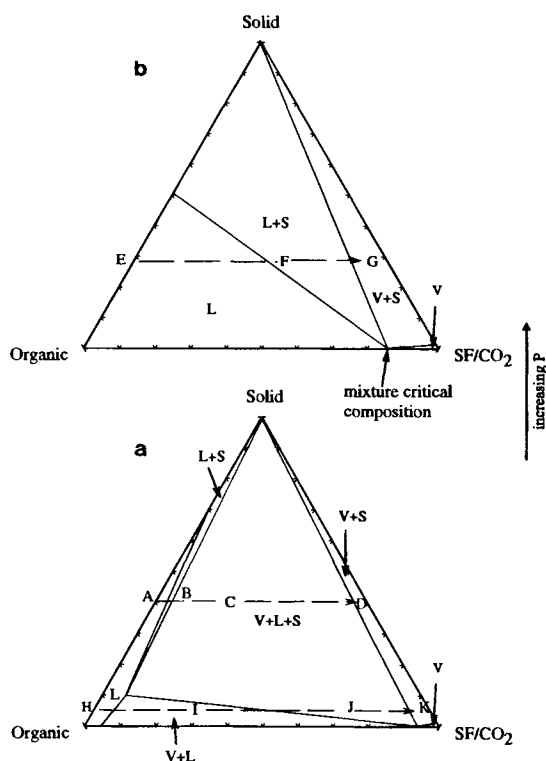


Fig. 5. Representative phase diagram of a ternary solid-organic solvent-SF system at constant temperature.

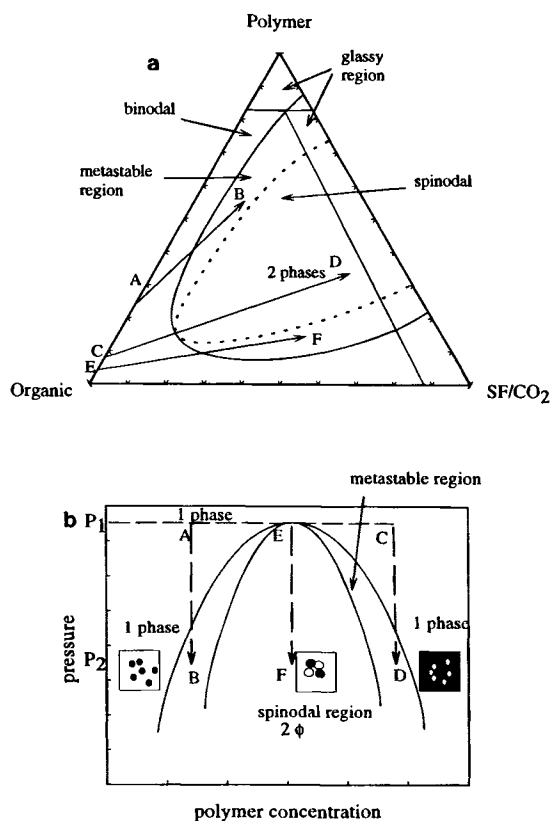


Fig. 6. (a) Representative diagram of a ternary polymer-organic solvent-SF system at constant temperature and pressure (after Dixon *et al.* (38)). (b) Schematic representation of a binary polymer-SF system showing different paths of Pressure Induced Phase Separation (PIPS) process along with different morphologies that could be obtained (after Kiran and Zhuang (39)).

phase region enveloped by the spinodal curve at constant temperature and pressure. At lower pressures the SF may exist as a separate vapour phase. Several examples of such polymer systems have been reported (1).

PARTICLE FORMATION PROCESSES WITH SUPERCRITICAL FLUIDS

Precipitation from Supercritical Solutions

As shown in Fig. 2, supercritical fluids exhibit remarkable dissolution power for certain low vapour pressure, high molecular weight compounds compared to gases at low pressures. The solvent strength can be manipulated by changing the SF density by altering the temperature and pressure. Thus by decreasing the solvent density and hence the solvent power, the solute precipitates from a homogeneous SF solution. This is often accomplished by rapidly expanding the SF solution across an orifice either under adiabatic, isothermal or isentropic conditions causing homogeneous nucleation. Such a process has been termed as Rapid Expansion of Supercritical Solutions (RESS) (22). The entire process is relatively simple and is shown schematically in Fig. 7a. Various compounds processed using the RESS technique include polymers, organic materials, steroids and a range of inorganics encompassing the chemical and

ceramic industries. The subject has been reviewed by several authors (10,23–25). The operating parameters affecting the particle characteristics are pre-expansion temperature and pressure, post-expansion temperature and pressure and the nozzle geometry.

Inorganic materials are often dissolved in SF water and hence the properties of the particles obtained on an expansion of such SF solutions are sensitive to the process path followed during expansion. An adiabatic expansion of an SF solution decreases the temperature dramatically. Matson and coworkers (26) report that a supercritical water solution of SiO_2 at pre-expansion temperature close to the critical point of pure water when expanded could intersect the saturated vapour curve, path A-B in Fig. 1a. Such conucleation of condensed liquid droplets along with the SiO_2 particles produces solid SiO_2 films. At sufficiently high pre-expansion temperatures and pressures ($T > 1.3T_c$ and $P > 5P_c$), i.e., the expansion path remote from the saturated vapour curve along C-D, the precipitation occurs in a homogeneous medium producing SiO_2 particles.

Similar morphological changes have been reported with SF-polymer systems. A phase separation at the pre-entry stage to the orifice, i.e. at conditions close to saturation, causes the polymer to precipitate as fibres (27). This situation can be induced by (a) high temperatures (density of the SF medium close to the saturation density) (b) high polymer concentrations (c) low pressure and (d) large opening orifices. While conditions (a), (b) and (c) are system dependent, the slower rate of expansion in wider orifices induce nucleation and growth. At conditions other than listed above, the solubility limits are reached in the orifice itself precipitating the polymer as particles in the free jet.

For organic compounds, expansion of SF solutions to relatively lower saturation limits, i.e., expanded to pressures greater than atmospheric levels, induces nucleation and growth leading to agglomerated particles (7). Unlike polymers, increased solute concentrations in SF solutions during expansion can cause high nucleation rates leading to smaller particles. In the presence of a modifier, expansion of a SF solution in a single fluid phase occurs from conditions B to C in Fig. 3a without intersecting the saturated vapour curve. This results in smaller particles compared to conditions where the cosolvent and solute conucleate such as along the path of retrograde condensation D to E at 333 K (see Fig. 3a) (28).

Conucleation/coprecipitation of two solutes in a single process is often desirable, such as for the preparation of sustained release dosage forms. A drug embedded within the core of a polymer matrix diffuses out at a slower rate into the assimilating fluid in the body thereby giving a sustained therapeutic effect. Initial studies on the RESS process showed some promise in the coprecipitation of inorganics (26,29). Subsequently, Tom and Debenedetti coprecipitated DL-PLA and lovastatin (30) and L-PLA and pyrene (31) and found that the morphology of the resultant particles depends on the concentration of the drug/organic in the pre-expansion SF solution. While pyrene was found to be homogeneously distributed within the polymer matrix, lovastatin needles were embedded in the polymer. Kim and co-workers (32) showed that by carefully manipulating the operating variables, a more uniform coating of L-PLA over naproxen could be achieved.

While the RESS process is a versatile unit operation, its applicability in the pharmaceutical industry is limited in most

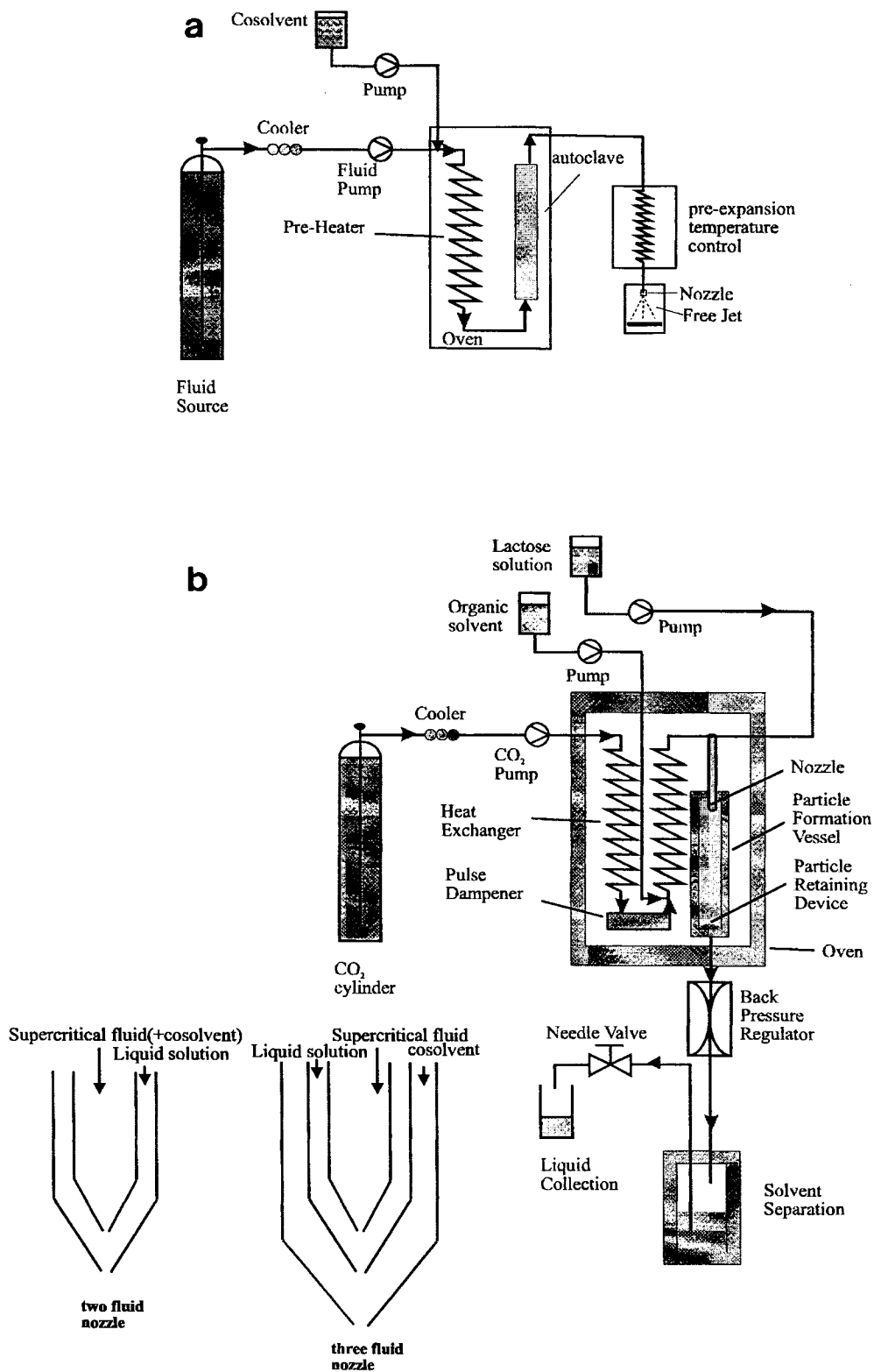


Fig. 7. (a) Schematic flow diagram of a RESS process. (b) Schematic flow diagram of a SEDS process along with a cross section of the two and three fluid nozzles.

cases due to very low or negligible solubility of most organics and biologicals in the commonly used SF CO₂. The use of other solvents as SF's is often restricted due to the strict regulations against the use of more toxic materials. Further, the high temperatures needed to avoid conucleation of the solvent along with the solute negates the potential advantage of low temperature processing with SF CO₂ compared to conventional methods.

PRECIPITATION WITH SUPERCRITICAL FLUIDS AS ANTISOLVENTS

High solubilities of SF's in organic solvents cause a volume expansion decreasing the densities up to a factor of 2 and consequently reducing the solvent capacity. Kordikowski and co-workers (33) reported volume expansion of several common organic solvents with different SF's dissolved in them. This concept has been employed to crystallise solutes insoluble in SF's from liquid solution and the process, termed as Gas Antisolvent (GAS) recrystallisation, was first applied to crystallise explosives (1). Several pharmaceutical compounds including drugs, biopolymers and proteins have since been prepared in fine particulate form using this technique (1,10–11,34). The operation is usually carried out in a batch mode by adding a SF to the liquid solution in an autoclave and allowing the solution to expand causing the solute to crystallise as micron sized particles. The process path, see Fig. 5, from concentrated solutions is along A-B-C-D at temperature and pressure conditions below the SF-solvent binary critical point and along the path E-F-G above the critical point. The path of precipitation from dilute solutions, such as H-I-J-K, is dependent on the rate of antisolvent addition and creates problems with nucleation, growth and particle agglomeration. Benedetti and co-workers (35) report that crystallisation from concentrated solutions gives 0.4 μm HYAFF polymer microspheres in contrast to fused particulate aggregates with dilute solutions. The GAS process was also deployed to coprecipitate HYAFF-11 polymer together with a steroid and protein by Bertuccio and co-workers (36). They observed that the steroid which is soluble in SF CO₂ precipitated on a core of polymer. In the GAS process the particles are essentially formed in the liquid phase and are dried in a final stage corresponding to paths B-D or J-K or F-G in Fig. 5. This requirement negates the benefits of rapid particle formation and the operation is carried out by flushing the system with pure SF for long periods of time, usually of the order of 2 hrs. Another problem associated with the GAS process is the dissipation of large amounts of heat generated due to rapid pressurisation and heat of mixing. Wubbolts and co-workers (37) report that the addition of carbon dioxide in a liquid phase instead of vapour or supercritical state to the mother liquor under helium pressure eliminates the problem of heat generation.

The GAS process had been modified into semi-continuous operation by spraying the liquid solution into a continuum of antisolvent fluid. The purpose is to contact small liquid solution droplets with a large excess of antisolvent in order to completely extract the organic solvent and thus form dry particles and reduce/eliminate the drying step of the GAS process. The technique termed Precipitation with Compressed Antisolvent (PCA) (38) utilises an antisolvent either in a liquid or supercritical state into which a liquid solution of polymer was dispersed through a fine capillary nozzle. Polystyrene was crystallised

from toluene and different morphologies were obtained by following different process paths in inducing a phase separation (38). For example, path A-B in Fig. 6a would intersect the metastable region in the polymer rich phase and path E-F would cross the polymer lean phase before vitrification resulting in nucleation and growth. As a result, the porosity of the polymer would increase as the path approaches the polymer lean phase. Path C-D would result in a rapid spinodal decomposition. Kiran and Zhuang (39) discuss the various factors influencing the polymer-SF miscibility and their effect on the phase separation.

In interesting studies with proteins, Tom and co-workers (30) and Yeo and co-workers (40) precipitated insulin and catalase into a continuum of supercritical carbon dioxide, calling the process Supercritical Antisolvent (SAS) precipitation. Although both PCA and SAS are similar, the rate of crystallisation within the droplet is a function of the rate of mass transfer of SF into the droplet. While this step determines the particle size, nucleation and agglomeration within each droplet is dependent on the concentration and rate of mass transfer of solvent into the SF phase. While the former phenomenon depends on the efficiency of droplet generation, the latter relies on the mixing characteristics within the bulk of SF phase. The droplet size depends on the Weber number (N_{We}) which is a ratio of the inertial and surface tension forces given by:

$$N_{We} = \rho_A v^2 D / \sigma \quad (1)$$

where ρ_A is the antisolvent density, v is the relative velocity, D is the jet diameter and σ is the interfacial tension. Thus, the higher the Weber number, the smaller the droplet size and vice versa (38). At temperature and pressure conditions above the mixture critical point of the solvent and SF antisolvent, the interfacial tension is zero. Thus in the miscible region, the droplet sizes are extremely small (Fig. 8aI). The rate of nucleation is therefore dependent on the saturation levels achieved by the rate of mass transfer of SF into the droplet which is a function of the diffusion coefficient of the SF in the solvent phase (Fig. 8aII). Thus, the higher the concentration of the solute within the droplet, the higher the nucleation rate with correspondingly less agglomeration. The next stage of solvent extraction into the SF phase (Fig. 8aIII) is again dependent on the mixing characteristics in the bulk phase and since the two fluids are miscible, the mass transport is a function of the diffusion coefficient of the solvent in the SF medium. The diffusion coefficient of acetone, for example, in SF CO₂ decreases with density (41). Hence, at higher densities of the SF medium, particle size could increase due to slower mass transfer of solvent. Such an effect of increase in particle size of L-PLA was reported by Randolph and co-workers (42) with an increase in CO₂ density. However, an opposite effect was observed by Mawson and co-workers (43) who found that the particle size of L-PLA increased with decreasing density of CO₂ at subcritical conditions. This phenomenon was attributed to larger droplet size due to lower antisolvent density.

At pressures below the binary SF-solvent mixture critical point, for example at P_{sub} at 333 K (Fig. 3a), the hydrodynamics and mass transfer mechanisms are quite different. At such conditions, as shown by the process path F-G in Fig. 3a, the two fluids are partially miscible. Thus the jet break up from the nozzle depends on the relative velocities and the interfacial tension. The density of such SF media, as shown in the representative plot for the ethanol-CO₂ system in Fig. 3b, is lower

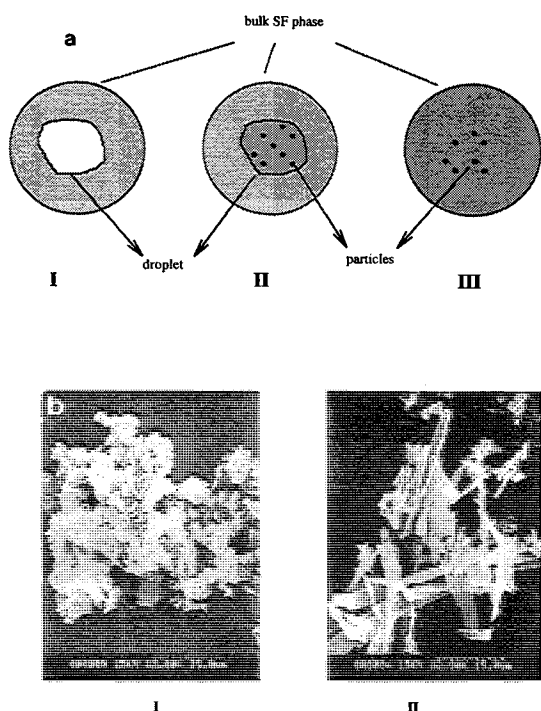


Fig. 8. (a) Schematic representation of (I) droplet formation (II) nucleation and (III) solvent evaporation. (b) Scanning electron micrographs of the SEDS processed lactose samples; flow rate of liquid CO_2 : (I) = 19.0 ml/min (II) = 5.0 ml/min (from Palakodaty *et al.* (53)).

compared to the single phase in the miscible region. From equation 1, the Weber number is small compared to values in the miscibility region consequently resulting in poor solution dispersion. The supersaturation levels with respect to the solute concentrations, obtained in the solvent rich phase, and the solvent extraction into the SF phase are limited by the mutual saturation solubility limits of the SF antisolvent and solvent. The rate of mutual transport of SF into the solvent rich phase and vice versa N_i (moles min^{-1}) is a function of the mass transfer coefficient and is given by the relation (44)

$$N_i = k_{L,SF} a (C_{i,e} - C) \quad (2)$$

where, a is the mass transfer area, $C_{i,e}$ is the equilibrium solubility in mole fraction units of the component i in the respective SF or liquid (L) phase, C is the concentration in mole fraction units at a particular instant of time. $K_{L,SF}$ (moles $\text{cm}^{-2} \text{min}^{-1}$ mole fraction $^{-1}$) is the overall mass transfer coefficient either in the liquid or SF phase which is a function of the system hydrodynamics and derived from the following correlation for flows in circular pipes (44) between the Sherwood number (Sh), Reynolds number (Re) and Schmidt number (Sc):

$$Sh_{L,SF} = c Re_{L,SF}^d Sc_{L,SF}^e \quad (3)$$

where c , d and e are system dependent constants.

Two ways of improving the mass transfer rates under such circumstances are (a) to maintain a significantly high ratio of the relative velocities of SF to the solvent and (b) increasing the SF to solvent ratio which increases the concentration gradient in equation (2). Such high ratio when coupled with high velocities of SF would also generate smaller droplet sizes giving an added

advantage. This concept was developed by Hanna and York (45) who incorporated a coaxial nozzle design with a mixing chamber to increase the relative velocity of the dispersing supercritical fluid. The process developed is called Solution Enhanced Dispersion by Supercritical Fluids (SEDS) and a schematic diagram of the nozzle along with the experimental set up is shown in Fig. 7b. The organic solution of a drug compound is contacted with the SF CO_2 in the mixing chamber of the nozzle before being dispersed through a narrow opening into a particle formation vessel. The high velocities of the SF CO_2 not only assist in breaking the liquid stream(s) and producing fine droplets but also improve the mixing characteristics in the vessel resulting in improved rates of solvent extraction, thereby providing a means of controlling the crystallisation mechanism. The process has been successful in preparing a range of organic materials including high purity polymorphic forms of salmeterol xinafoate—a drug compound used in the treatment of asthma (46–47). In later work, Jaarmo and co-workers (48) crystallised the anti allergic agent sodium cromoglycate from methanol in both amorphous and crystalline forms using the same principle. Another study reported, using a coaxial nozzle without a mixing chamber (43), crystallised L-PLA, polystyrene and polyacrylonitrile (PAN). In contrast to the single fluid nozzle, as was used in earlier work with PCA process, the authors observed low Weber numbers with the coaxial nozzle resulting in larger droplets and consequently a delayed precipitation. Owing to such a delay in precipitation, PAN was observed to crystallise as microparticles as opposed to fibrils when prepared by using the single fluid nozzle. However, increased velocities in the suspension outside the jet increased the mass transfer of the solvent into the SF phase thereby decreasing the degree of flocculation and agglomeration.

Crystallisation from aqueous solutions using SF CO_2 is difficult due to the limited solubility of carbon dioxide in water and vice versa. Also, pH of the aqueous medium in contact with SF CO_2 is usually between 2.5–3, which would be unfavourable for processing labile protein molecules. One approach is to use an organic solvent, which is a poor solvent for the solute in conjunction with the SF. The cosolvent is then distributed into the aqueous phase along with the SF, but limited by the equilibrium concentration values as shown by the tie lines in Fig. 4. The ratio of SF + cosolvent:water determines the saturation levels with respect to the solute causing nucleation. Tom and coworkers (30), in their study on the crystallisation of insulin and catalase from 90:10 ethanol-water solution with SF CO_2 using the SAS process, observed two different particle morphologies within the crystallised product. Difficulties in product collection due to the residual water were reported. Palakodaty and co-workers (49) crystallised α -lactose monohydrate with a uniform morphology of thin long bands from a 95:5 methanol-water solution using the SEDS process.

Such procedures of precipitating solutes from organic rich phases is not generally suitable for macromolecules like proteins which may be denatured in the presence of organic solvents. Hanna and York (50) developed a three fluid coaxial nozzle to crystallise compounds from aqueous solutions with the aqueous solution, organic antisolvent and SF antisolvent streams fed independently into three concentric annuli. The three fluids are contacted in a mixing chamber within the nozzle (see Fig. 7b) thereby minimising the contact time between the labile macromolecules, such as proteins, and the organic solvent prior

to nucleation and particle formation. Sloan and co-workers (51) successfully used the three fluid nozzle in precipitating lysozyme and trypsin with the SEDS process. Palakodaty and coworkers (52) compared the performance of the SEDS two and three fluid nozzles by crystallising α -lactose monohydrate and reported that the rate of crystallisation and particle morphology can be controlled by the choice of the nozzle. In a more detailed study (53), it was shown that the particle morphology of α -lactose monohydrate could be modified by altering the process path using a two fluid nozzle. An aqueous solution was dispersed with a homogeneous phase of CO_2 + cosolvent mixture at various flow rates of SF CO_2 at different temperature and pressure conditions. At a constant ratio of water to organic cosolvent, the distribution of the cosolvent between the aqueous phase and CO_2 rich phase changes with the amount of CO_2 present in the system as shown by the tie lines in Fig. 4. At low flow rates/concentrations of CO_2 , the three fluids are completely miscible and lactose crystallised at a rapid rate as thin long bands (see Fig. 8b) due to high supersaturation. On the other hand, at high CO_2 flows, the cosolvent is more selective towards the CO_2 rich phase and the crystallisation is slower in the aqueous phase giving rise to growth and agglomeration of the lactose particles as shown in Fig. 8b.

PRECIPITATION FROM GAS SATURATED SOLUTIONS

Another type of crystallisation process involving aspects of solute-SF miscibility is precipitation from gas saturated solutions. Here, a supercritical fluid is dissolved in a molten solute and the high pressure SF saturated solution is expanded through a nozzle to atmospheric conditions (54). In principle, the technique is similar to the RESS process except that on expansion the phase separation is caused by evaporation of the volatile component from the homogeneous liquid phase. In addition to crystallising polyethylene glycols, it has been demonstrated that the process is viable in producing micron sized particles of nifedipine and a coformulation of nifedipine with PEG 4000 (55). While the technique is simple and efficient in producing particles, the high temperatures involved in melting the solute makes the process infeasible for processing most pharmaceuticals, especially, thermally labile compounds.

A process similar in principle—Pressure Induced Phase Separation (PIPS) (39) is reported where a homogeneous solution of polymer + SF, either in the liquid or supercritical state is expanded in a controlled operation in a batch mode. The quality of the resultant polymer particle can be manipulated by adjusting the rate of pressure reduction. A binodal curve of a binary polymer-SF system is shown in Fig. 6b along with the metastable region. Homogeneous solutions of different concentrations when depressurised across the same pressure gradient undergo phase transitions either in the metastable region (polymer lean phase, path A-B or polymer rich phase path C-D) or pass through a spinodal decomposition, path E-F. A schematic description of the separated phases is also shown in Fig. 6b. A polymer lean phase separation is characterised by polymer separation from a continuous SF phase. In the spinodal region, the two phases are interconnected by a network while in the polymer rich phase, the SF phase is separated from a continuous polymer phase. Thus, porosity of the separated polymer rises with increased concentration in the initial solution for the same

gradient of pressure decrease. A homogeneous solution of a ternary system of solvent-polymer-SF solution can be depressurised in a controlled manner into two phases—polymer phase and solvent + SF phase. An understanding of the ternary system phase behaviour can thus be of significant value in controlled drug release applications in preparing a porous polymer matrix with an incorporated drug.

CONCLUSIONS

Materials processing with supercritical fluids has enormous potential for pharmaceutical compounds. Precipitation from supercritical solutions is often limited by the solute solubility in the supercritical fluid. The pressure reduction path can be designed to achieve phase separation in the free jet and avoiding precipitation of the SF solvent and the cosolvent. Thus, this process is highly dependent on the nozzle geometry. The continuous GAS processes are limited by the mutual mass transport of SF into solvent and vice versa. Faster nucleation, smaller particle size with less agglomeration is a characteristic feature of crystallisation occurring at conditions of high solute concentration in solvent, high mass transfer of SF into solvent and also high rates of solvent transfer into the SF phase. These conditions are generally prevalent in the SF rich phase of the SF-solvent miscibility region. At conditions below the mixture critical point, the mutual mass transport depends on the degree of mixing. A suitably designed nozzle can be deployed to achieve this requirement. With a high degree of solvent extraction achieved in the vessel, the SF process becomes particularly favourable for processing macromolecules from aqueous solutions. The process path chosen in the case of precipitating polymers is especially crucial, as the porosity changes are sensitive to the physical state of the precipitating medium. This feature is particularly important in incorporating a drug substance in the polymer matrix for controlled release applications.

Thus, a thorough understanding of the relevant phase behaviour and the mass transport characteristics gives the flexibility of fine tuning the SF processes to give particles with defined morphological and physico chemical characteristics.

REFERENCES

1. M. A. McHugh and V. J. Krukoni. *Supercritical Fluid Extraction. Principles and Practice* 2nd Edition, Butterworth-Heinemann, USA, 1994.
2. S. Angus, B. Armstrong, and K. De Reuk. *International thermodynamic tables of the fluid state-3. Carbon dioxide (Volume 3)*. Pergamon Press, 1976.
3. K. Stephan and K. Lucas. *Viscosity of dense fluids*. Plenum Press, New York, 1979.
4. J. M. Dobbs, J. M. Wong, and K. P. Johnston. Nonpolar cosolvents for solubility enhancement in supercritical carbon dioxide. *J. Chem. Eng. Data*. **31**:303–308 (1986).
5. J. M. Dobbs, J. M. Wong, R. J. Lahiere, and K. P. Johnston. Modification of supercritical fluid phase behaviour using polar cosolvents. *Ind. Eng. Chem. Res.* **26**:56–65 (1987).
6. J. G. Van Alsten and C. A. Eckert. Effect of entrainers and of solute size and polarity in supercritical fluid solutions. *J. Chem. Eng. Data*. **38**:605–610 (1993).
7. P. Alessi, A. Cortessi, I. Kikic, N. R. Foster, S. J. Macnaughton, and I. Combo. Particle production of steroid drugs using supercritical fluid processing. *Ind. Eng. Chem. Res.* **35**:4718–4726 (1996).
8. S. S. T. Ting, S. J. Macnaughton, D. L. Tomasko, and N. R. Foster. Solubility of naproxen in supercritical carbon dioxide with and without cosolvents. *Ind. Eng. Chem. Res.* **32**:1471–1481 (1993).

9. Z. Knez, M. Skerget, P. Sencar-Bozic, and A. Rizner. Solubility of nifedipine and nitrendipine in supercritical CO₂. *J. Chem. Eng. Data*. **40**:216–220 (1995).
10. B. Subramaniam, R. A. Rajewski, and K. Snavely. Pharmaceutical processing with supercritical carbon dioxide. *J. Pharm. Sci.* **86**:885–890 (1997).
11. I. Kikic and P. Sist. Applications of supercritical fluids to pharmaceuticals: Controlled drug release systems. *2nd NATO ASI on Supercritical Fluids*, Kemer, Turkey, 1998.
12. H. Tanaka and M. Kato. Vapour-liquid equilibrium properties of carbon dioxide + ethanol mixture at high pressures. *J. Chem Eng. Jap.* **28**:263–266 (1995).
13. K. Suzuki, H. Sue, M. Itou, R. L. Smith, H. Inmata, K. Arai, and S. Saito. Isothermal vapour-liquid equilibrium data for binary systems at high pressures: Carbon dioxide-methanol, carbon dioxide-ethanol, carbon dioxide-1-propanol, methane-ethanol, methane-1-propanol, ethane-ethanol and ethane-1-propanol systems. *J. Chem. Eng. Data*. **35**:63–66 (1990).
14. DECHEMA Chemistry Data Series, 1981.
15. S. Ohe. *Vapour-liquid equilibrium data at high pressure*. Elsevier, Japan, 1990.
16. R. E. Fornari, P. Alessi, and I. Kikic. High pressure fluid phase equilibria: Experimental methods and systems investigated (1978–1987). *Fluid Phase Equilibria*. **57**:1–33 (1990).
17. R. Dohrn and G. Brunner. High-pressure fluid phase equilibria: Experimental methods and systems investigated (1988–1993). *Fluid Phase Equilibria*. **106**:213–282 (1995).
18. M. L. Gilbert and M. E. Paulaitis. Gas-liquid equilibrium for ethanol-water-carbon dioxide mixtures at elevated pressures. *J. Chem. Eng. Data*. **31**:296–298 (1986).
19. S. Yao, Y. Guan, and Z. Zhu. Investigation of phase equilibrium for ternary systems containing ethanol, water and carbon dioxide at elevated pressures. *Fluid Phase Equilibria*. **99**:249–259 (1994).
20. G. Brunner. *Gas Extraction: An introduction to fundamentals of supercritical fluids and the application to separation processes*. Springer, New York, 1994.
21. R. G. Wissinger and M. E. Paulaitis. Glass transitions in polymer/CO₂ mixtures at elevated pressures. *J. Pol. Sci. B*. **29**:631–633 (1991).
22. D. W. Matson, R. C. Peterson, and R. D. Smith. Production of fine powders by the rapid expansion of supercritical fluid solutions. *Adv. In Ceramics*. **21**:109 (1987).
23. J. W. Tom and P. G. Debenedetti. Particle formation with supercritical fluids-A Review. *J. Aerosol. Sci.* **22**:555–584 (1991).
24. E. M. Philips and V. J. Stella. Rapid expansion from supercritical solutions: application to pharmaceutical processes. *Int. J. Pharm.* **94**:1–10 (1993).
25. B. L. Knutson, P. G. Debenedetti, and J. W. Tom. In S. Cohen, H. Bernstein (eds.), *Microparticulate systems for the delivery of proteins and vaccines, Drugs and the Pharmaceutical Sciences Series*, Marcel Dekker Inc., New York, 1996, 77, 89–125.
26. D. W. Matson, K. A. Norton, and R. D. Smith. Making powders and films from supercritical solutions. *CHEMTECH*, **8**:480–486 (1989).
27. A. K. Lele and A. D. Shine. Morphology of polymers precipitated from a supercritical solvent. *AIChE J.* **38**:742–752 (1992).
28. C. J. Chang and A. D. Randolph. Precipitation of microsize organic particles from supercritical fluids. *AIChE J.* **35**:1876–1882 (1989).
29. D. W. Matson, C. R. Petersen, and R. D. Smith. Production of powders and films by the Rapid Expansion of Supercritical Solutions. *J. Mat. Sci.* **22**:1919–1928 (1987).
30. J. W. Tom, G. Lim, P. G. Debenedetti, and R. K. Prud'homme. Applications of supercritical fluids in the controlled release of drugs. *ACS Symp. Series*. **514**:238–257 (1993).
31. J. W. Tom and P. G. Debenedetti. Precipitation of poly(L-lactic acid) and composite poly(L-lactic acid)-pyrene particles by rapid expansion of supercritical solutions. *J. Supercrit. Fluids*. **7**:9–29 (1994).
32. J. H. Kim, T. E. Paxton, and D. L. Tomasko. Microencapsulation of naproxen using Rapid Expansion of Supercritical Solutions. *Biotechnol Prog.* **12**:650–661 (1996).
33. A. Kordikowski, A. P. Schenk, R. M. Van Nielen and C. J. Peters. Volume expansions and vapour-liquid equilibria of binary mixtures of a variety of polar solvents and certain near-critical solvents. *J. Supercrit. Fluids*. **8**:205–216 (1995).
34. E. Reverchon. Supercritical antisolvent precipitation: Its application to microparticle generation and products fractionation. In *Proceedings of the 5th Meeting on Supercritical Fluids*. Materials and Natural products processing. Nice, France, 1998, Tome 1, pp. 221–236.
35. L. Benedetti, A. Bertucco, and P. Pallado. Production of micronic particles of biocompatible polymer using supercritical carbon dioxide. *Biotechnol. Bioeng.* **53**:232–237 (1997).
36. A. Bertucco, P. Pallado, and L. Benedetti. Formation of biocompatible polymer microspheres for controlled drug delivery by a supercritical antisolvent technique. In Ph. R. Von Rohr and Ch. Trepp (eds.), *Process Technology Proceedings, 12, High Pressure Chemical Engineering*, Elsevier, Netherlands, 1996, pp. 217–222.
37. F. E. Wubbolts, C. Kersch, and V. Rosmalen. Semi-batch precipitation of acetaminophen from ethanol with liquid carbon dioxide at a constant pressure. In *Proceedings of the 5th Meeting on Supercritical Fluids*. Materials and natural products processing. Nice, France, 1998, Tome 1, pp. 249–256.
38. D. J. Dixon, K. P. Johnston, and R. A. Bodmeier. Polymeric materials formed by precipitation with a compressed fluid antisolvent. *AIChE J.* **39**:127–139 (1993).
39. E. Kiran and W. Zhuang. Miscibility and phase separation of polymers in near-and supercritical fluids. *ACS Symposium Series*. **670**:2–36 (1997).
40. S. D. Yeo, G. Lim, P. G. Debenedetti, and H. Bernstein. Formation of microparticulate protein powders using a supercritical fluid antisolvent. *Biotechnol. Bioeng.* **41**:341–346 (1993).
41. P. R. Sassiati, P. Mourier, M. H. Caude, and R. H. Rosset. Measurement of diffusion coefficients in supercritical carbon dioxide and correlation with the equation of Wilke and Chang. *Anal. Chem.* **59**:1164–1170 (1987).
42. T. W. Randolph, A. D. Randolph, M. Mebes, and S. Yeung. Sub micrometer sized biodegradable particles of poly(L-lactic acid) via the gas antisolvent spray precipitation process. *Biotechnol. Progr.* **9**:429–435 (1993).
43. S. Mawson, S. Kanakia, and K. P. Johnston. Coaxial nozzle for control of particle morphology in precipitation with a compressed fluid antisolvent. *J. Appl. Pol. Sci.* **64**:2105–2118 (1997).
44. R. E. Treybal. *Mass transfer operations*. McGraw Hill, USA, 1980.
45. M. Hanna and P. York. Method and apparatus for the formation of particles. Patent No: *PCT/GB94/01426*. 1994.
46. M. Hanna and P. York. Particle engineering by supercritical fluid technologies for powder inhalation drug delivery. In *Proceedings of Respiratory Drug Delivery V*, Pheonix, USA, 1996, pp. 231–239.
47. M. Hanna, P. York, and B. Y. Shekunov. Control of the polymorphic forms of a drug substance by solution enhanced dispersion by supercritical fluids (SEDS). In *Proceedings of the 5th Meeting on Supercritical Fluids*. Materials and natural products processing. Nice, France, 1998, Tome 1, pp. 325–330.
48. S. Jaarmo, M. Rantakyla, and O. Aaltonen. Particle tailoring with supercritical fluids: Production of amorphous pharmaceutical particles. In *Proceedings of the 4th International Symposium on Supercritical Fluids*, Sendai, Japan, 1997, pp. 263–266.
49. S. Palakodaty, M. Hanna, P. York, D. Rudd, and J. Pritchard. Particle formation using Supercritical fluids—A novel approach. In Proc. 1997 *ICHEME Event*, UK. ISBN: 0 85295 389 5, 1:501–504 (1997).
50. M. Hanna and P. York. Method and apparatus for the formation of particles. Patent No.: *PCT/GB95/01523*. 1995.
51. R. Sloan, M. E. Hollowood, W. Ashraf, P. York, and G. O. Humphreys. Supercritical fluid processing: Preparation of stable protein particles. In *Proceedings of the 5th Meeting on Supercritical Fluids*. Materials and natural products processing. Nice, France, 1998, Tome 1, pp. 301–306.
52. S. Palakodaty, J. Pritchard, P. York, and M. Hanna. Crystallisation of lactose using solution enhanced dispersion by supercritical fluid (SEDS) technique. In *Proceedings of the 5th Meeting on Supercritical Fluids*. Materials and natural products processing. Nice, France, 1998, Tome 1, pp. 275–280.

53. Palakodaty, P. York, and J. Pritchard. Supercritical fluid processing of materials from aqueous solutions: The application of SEDS to lactose as a model substance. *Pharm. Res.* In press. (1998).
54. E. Weidner, R. Steiner, and Z. Knez. Powder generation from polyethyleneglycols with compressible fluids. In Ph. R. Von Rohr and Ch. Trepp (eds.), *Process Technology Proceedings 12, High Pressure Chemical Engineering*, Elsevier, Netherlands, 1996, pp. 223–228.
55. S. Srcic, P. Sencar-Bozic, Z. Knez, and J. Kerc. Improvement of nifedipine dissolution characteristics using supercritical CO₂. *Proceedings of the 16th Pharmaceutical Technology Conference and Exhibition*, Athens, Greece. 1997, pp. 59–69.